# 3-Bromopyruvate Induces Endoplasmic Reticulum Stress, Overcomes Autophagy and Causes Apoptosis in Human HCC Cell Lines

SHANMUGASUNDARAM GANAPATHY-KANNIAPPAN*, JEAN-FRANCOIS H. GESCHWIND*, RANI KUNJITHAPATHAM*, MANON BUIJS, LABIQ H. SYED, PRAMOD P. RAO, SHINICHI OTA, BYUNG KOOK KWAK, ROMARIC LOFFROY and MUSTAFA VALI

*Russell H. Morgan Department of Radiology and Radiological Sciences, Johns Hopkins University School of Medicine, Baltimore, MD 21287, U.S.A.*

**Abstract.** *Background: Autophagy, a cellular response to stress, plays a role in resistance to chemotherapy in cancer cells. Resistance renders systemic chemotherapy generally ineffective against human hepatocellular carcinoma (HCC). Recently, we reported that the pyruvate analog 3-bromopyruvate (3-BrPA) promoted tumor cell death by targeting GAPDH. In continuance, we investigated the intracellular response of two human HCC cell lines (Hep3B and SK-Hep1) that differ in their status of key apoptotic regulators, p53 and Fas. Methods and Results: 3-BrPA treatment induced endoplasmic reticulum (ER) stress, translation inhibition and apoptosis based on Western blot and qPCR, pulse labeling, Terminal deoxynucleotidyl transferase dUTP nick end labeling (TUNEL) assay and active caspase-3 in both the cell lines. However, electron microscopy revealed that 3-BrPA treated SK-Hep1 cells underwent classical apoptotic cell death while Hep3B cells initially responded with the protective autophagy that failed to prevent eventual apoptosis. Conclusion: 3-BrPA treatment promotes apoptosis in human HCC cell lines, irrespective of the intracellular response.*

The ability of cancer cells to evade apoptosis is a key mechanism contributing to the uncontrolled growth and resistance to therapy (1). The emerging reports emphasize the influence of autophagy as a process that regulates the survival of cancer cells. Autophagy could be either tumor suppressive or tumor promoting functions (2, 3). The autophagic mechanisms have been categorized into microautophagy, chaperone-mediated autophagy and macroautophagy. Macroautophagy is by far the best understood process in cancer cells and has been shown to play a role in resistance to chemotherapy (4). Cellular stress, particularly endoplasmic reticulum (ER) stress is one of the factors that can influence autophagy (3, 5). ER is the principal organelle that provides cytoskeletal structure and is the site of protein synthesis and folding. Various cellular conditions, such as energy depletion, increased demand for protein synthesis, accumulation of misfolded proteins, perturbations in $Ca^{2+}$ homeostasis and altered glycosylation, affect the intracellular environment, resulting in the ER stress. There are three types of consequences to triggering ER stress, namely adaptation, alarm and apoptosis (6). When the adaptive mechanisms fail to compensate, cell death is induced, mostly by apoptosis. However, it is clear that the cell death mechanisms triggered as a result of ER stress are diverse, involving both caspase-dependent apoptosis and caspase-independent necrosis (7). Recent reports show that ER stress induces autophagy (8, 9), which has been associated with induction of apoptotic and non-apoptotic cell death in cancer cells (10).

Hepatocellular carcinoma (HCC) is an aggressive form of cancer and is the fifth most common cause of cancer death worldwide. Surgical resection is the only curative treatment but its feasibility is limited to very few patients as most HCC patients are diagnosed at an advanced stage of disease (11). HCC is resistant to systemic chemotherapy and this resistance has been attributed to several complex mechanisms, one of which is dysfunctional apoptotic machinery (12, 13). The significance of key apoptotic regulators in influencing the therapeutic efficacy is well

*These authors contributed equally to this study.

*Correspondence to:* Dr. Jean-Francois Geschwind, Russell H. Morgan Department of Radiology and Radiological Sciences, Johns Hopkins University School of Medicine, 600 N. Wolfe Street, Blalock Building, Room 545, Baltimore, MD 21287, U.S.A. Tel: +14109557043, Fax: +14109550233, e-mail: jfg@jhmi.edu

*Key Words:* ER stress, antiglycolytic, autophagosome, translation inhibition.

documented (11). Human HCC cell line Hep3B is deficient in the expression of the gene *p53* (14), hence Hep3B cells are insensitive to p53-dependent apoptosis. The ectopic expression of p53 in Hep3B cells does not restore the p53-dependent apoptotic pathway, implying that the other effector molecules involved in the pathway are also impaired. It has also been reported that the resistance of Hep3B cells to Fas-ligand based apoptotic pathways is due to the dysfunctional Fas/CD95 surface receptor (15). In contrast, SK-Hep1 cells, which express wild-type p53 and Fas, show less resistance and are sensitive to cell death by the classic apoptotic pathway. Muller *et al*. (16) have provided evidence on the links of p53 and Fas ligand with apoptotic events in liver tumors treated with chemotherapeutic agents. However, p53-deficient cells still exhibit apoptosis through other p53-independent apoptotic pathways (17).

The pyruvate analog, 3-bromopyruvate (3-BrPA) is an antiglycolytic agent that alkylates GAPDH to cause ATP depletion in cancer cells, resulting in apoptosis both in *in vitro* and *in vivo* (18-21). GAPDH is a glycolytic enzyme that has been shown to be involved in multiple diversified cellular functions (22). GAPDH is cell cycle-dependently expressed in normal cells but significantly overexpressed in cancer cells (23). Alkylation of GAPDH has been shown to cause apoptosis in a variety of cancer cell lines (20).

In this study, we compared the intracellular responses of Hep3B to SK-Hep1 cells on treatment with 3-BrPA.

## Materials and Methods

*Cell lines, chemicals and antibodies*. HCC cell lines Hep3B and SK-Hep1 were obtained from the ATCC (Manassas, VA, USA) and were cultured according to their instructions. Unless otherwise mentioned, all the chemicals including 3-BrPA were obtained from Sigma Chemical Co. (St Louis, MO, USA). Primers were synthesized at Johns Hopkins University DNA synthesis core facility (Baltimore, MD, USA). The antibodies for phospho-stress-activated protein kinase (SAPK) / Jun *N* terminal kinase (JNK), S6 ribosomal protein, heat shock protein 27 (HSP 27), total and phospho-eukaryotic initiation factor 2α (eIF2α), α-tubulin, binding protein (BiP), protein kinase-like endoplasmic reticulum kinase (PERK), protein disulfide isomerase (PDI), calnexin, endoplasmic oxidoreductin-1α (Ero1α), inositol-requiring enzyme-1α (IRE1α), autophagy-related (ATG) proteins ATG5 and ATG7 were purchased from Cell Signaling Technology (Danvers, MA, USA) and anti- C/EBP α homologous protein (CHOP), anti-ubiquitin and anti-active caspase-3 were procured from Novus Biologicals Inc., (Littleton, CO, USA). ECL Plus detection reagent and the necessary materials for autoradiography were all purchased from GE-Healthcare (Piscataway, NJ, USA). All the other reagents including NuPAGE Bis-Tris gels, electrophoretic and blot transfer-associated reagents (Invitrogen, Carlsbad, CA, USA), BCA protein assay kit (Pierce Co., Rockford, IL, USA),TUNEL assay kit (Millipore Inc., Danvers, MA, USA), Cell Titer Glo-ATP viability assay kit (Promega Co., San Luis Obispo, CA, USA), [$^{35}$S] methionine (Perkin Elmer Co., Waltham, MA, USA), were obtained from the respective manufacturers.

Table I. *Primer sequences used for qRT-PCR*.

| Gene symbol | | Sequence |
|---|---|---|
| *ATF4* | (forward) | 5' CTTACGTTGCCATGATCCCT 3' |
| | (reverse) | 5' CTTCTGGCGGTACCTAGTGG 3' |
| *ACTB* | (forward) | 5' TCCTCCCTGGAGAAGAGCTAC 3' |
| | (reverse) | 5' TCCTGCTTGCTGATCCACAT 3' |
| *BiP* | (forward) | 5' GTTTGCTGAGGAAGACAAAAAGCTC 3' |
| | (reverse) | 5' CACTTCCATAGAGTTTGCTGATAAT 3' |
| *CHOP* | (forward) | 5' CAGAACCAGCAGAGGTCACA 3' |
| | (reverse) | 5' AGCTGTGCCACTTTCCTTTC 3' |
| *GADD 34* | (forward) | 5' GTGGAAGCAGTAAAAGGAGCAG 3' |
| | (reverse) | 5' CAGCAACTCCCTCTTCCTCG 3' |
| *XBP1* | (forward) | 5' AAACAGAGTAGCAGCTCAGACTGC 3' |
| | (reverse) | 5' TCCTTCTGGGTAGACCTCTGGGAG 3' |

*Quantitative RT-PCR (qRT-PCR) and immunoblotting*. Total RNA was extracted using RNeasy kit (QIAGEN) and then subjected to reverse transcription (RT)-PCR using High Capacity cDNA Reverse Transcription kit (Applied Biosystems Inc., Bedford, MA, USA). The cDNAs were amplified with specific primers for alternative transcription factor 4 (ATF4), BiP, CHOP, growth arrest and DNA damage 34 (GADD 34) and x-box binding protein1 (XBP1) that were designed based on published literature (Table I). The 18S primers for internal control were obtained from Applied Biosystems Inc. Immunoblotting was performed using the whole-cell lysates as described previously (20) and the antibody incubation procedures were followed as per the manufacturer's instructions.

*Determination of protein synthesis by metabolic labeling (pulse) experiment*. 3-BrPA treated cells were pulse-labeled with [$^{35}$S] methionine (100 μCi/ml) for different time periods, washed in ice-cold phosphate- buffered saline (PBS), and lysed in ice-cold radioimmunoprecipitation assay (RIPA) buffer supplemented with protease and phosphatase inhibitors. In brief, cells growing in log phase were counted and plated on the previous day of experiment. On the day of experiment, cells were left in Opti-MEM for 6 h, followed by treatment with either 3-BrPA (100 μM, 200 μM) or the vehicle (as control) for 60 min. At specified times, the medium was removed and [$^{35}$S] methionine-containing regular growth medium was added for different time intervals (30, 60 and 120 min). The cells were then harvested and lysed in RIPA buffer for further analyses. Radioactive waste disposal was performed in accordance with the Johns Hopkins Radiation Safety protocol. Protein samples from the cell lysates were separated on 4-12% NuPAGE Bis-Tris denaturing gel, stained with colloidal Coomassie brilliant blue (24) and the gel images were scanned before drying the gel for autoradiography.

*Electron microscopy*. The cells grown on petri-dishes were fixed in 2% glutaraldehyde in 0.1 M cacodylate with 3 mM $CaCl_2$ at 4˚C overnight and post-fixed for 60 min with reduced osmium tetroxide. The cells were dehydrated through graded ethanol and embedded in Eponate 12 Resin (Ted Pella Inc., Redding, CA, USA). The thin sections were placed on 200 mesh copper grids and stained with uranyl acetate followed by lead citrate. The grids were examined on a Hitachi 7600 transmission electron microscope.

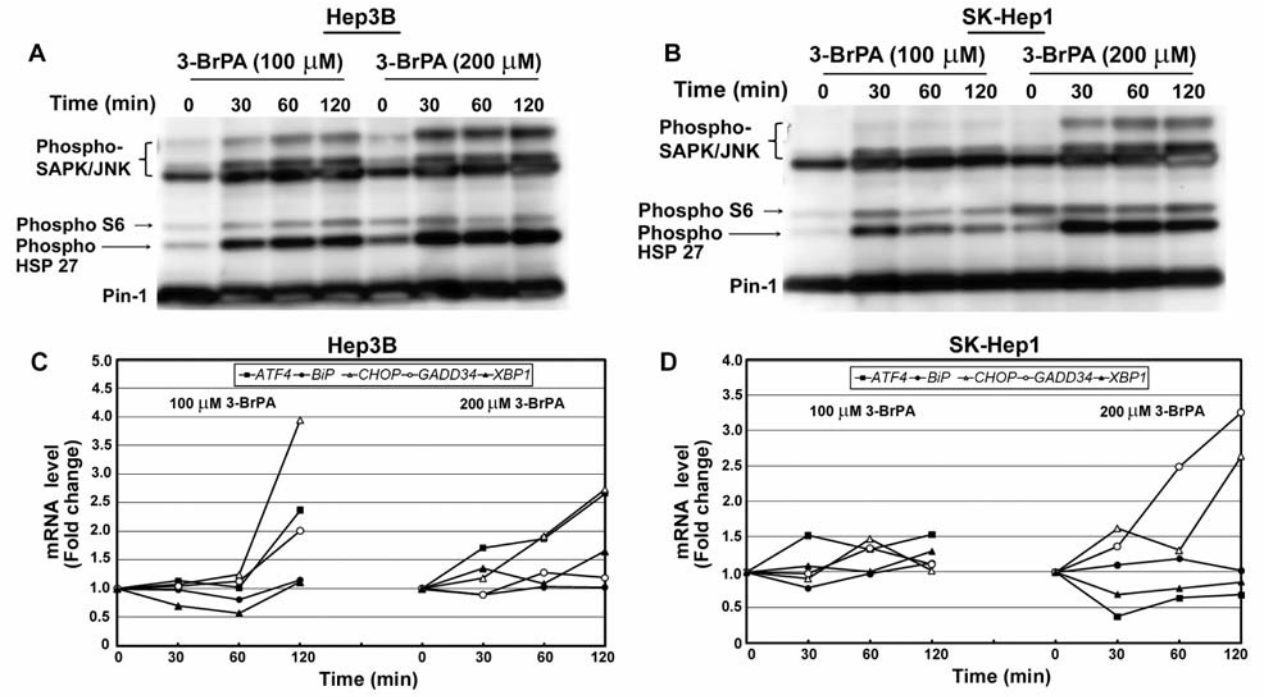


Figure 1. *3-BrPA treatment induced cellular stress in HCC cell lines. Immunoblots of Hep3B (A) and SK-Hep1 (B) cells showing a dose- and time-dependent increase in stress markers such as phosphorylated SAPK/JNK, S6 ribosomal protein and HSP 27. Pin-1 served as a loading control. qRT-PCR showing 3-BrPA-mediated induction of ER stress markers in Hep3B (C) and SK-Hep1 (D) cells. Hep3B cells showed cellular stress activation and early onset of ER stress (100 μM 3-BrPA) compared to SK-Hep1 cells (200 μM 3-BrPA). Data represent mean values of triplicates.*

*Quantification of intracellular ATP.* The cells treated with different concentrations of 3-BrPA for the indicated time intervals were assayed for the intracellular ATP level. The cells growing in log phase were plated in 96-well, flat-bottomed opaque plates the day before 3-BrPA treatment. At the end of the treatment, the quantity of ATP was measured using a Cell Titer-Glo kit (Promega Co.) in a Victor$^3$-multilabel plate reader. The cell viability, or cytotoxicity, was also confirmed by the vital stain (Trypan blue exclusion) method.

*Apoptosis assays*. The apoptosis of 3-BrPA-treated cells was evaluated by terminal deoxynucleotidyl transferase dUTP nick-end labeling (TUNEL) assay and the level of caspase-3 activation by immunoblotting. Cells treated with 3-BrPA were stained for TUNEL assay as per manufacturer's instructions and the fluorescent images were captured in a Zeiss Axiovert 200 Microscope (Carl Zeiss Microimaging Inc., Thornwood, NY, USA). The activation of caspase-3 was determined by subjecting the lysates obtained from cells treated with different concentrations of 3-BrPA and control to immunoblotting technique.

## Results

*3-BrPA treatment induced ER stress*. First, we tested the effect of 3-BrPA treatment on intracellular stress of Hep3B and SK-Hep1 cells. 3-BrPA treatment induced the intracellular stress markers as evident from the increased level of phosphorylated SAPK/JNK, HSP 27 and S6

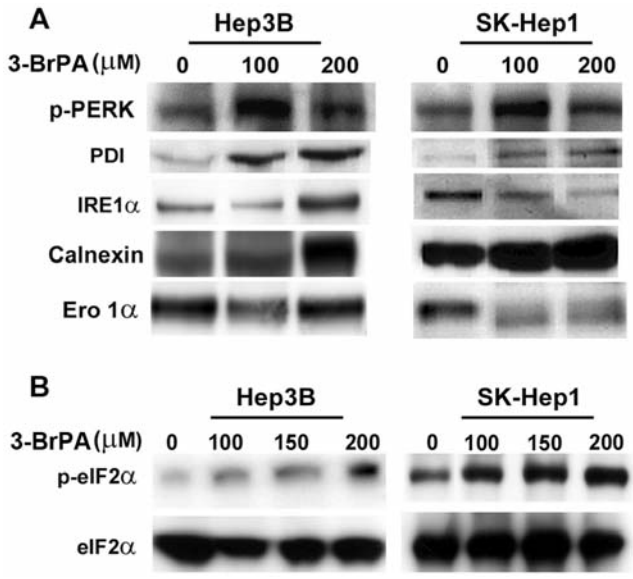


Figure 2. *Differential expression of ER stress markers in HCC cell lines induced by 3-BrPA treatment. A: Immunoblots showing an increase in phospho-PERK, PDI, Calnexin in both Hep3B and SK-Hep1 cells, whereas IRE1α and Ero1 increased only in Hep3B cells. B: 3-BrPA treatment increased the phosphorylation of eIF2α in a dose-dependent manner in both Hep3B and SK-Hep1 cells. The same membrane was reprobed with different antibodies to acheive loading control.*

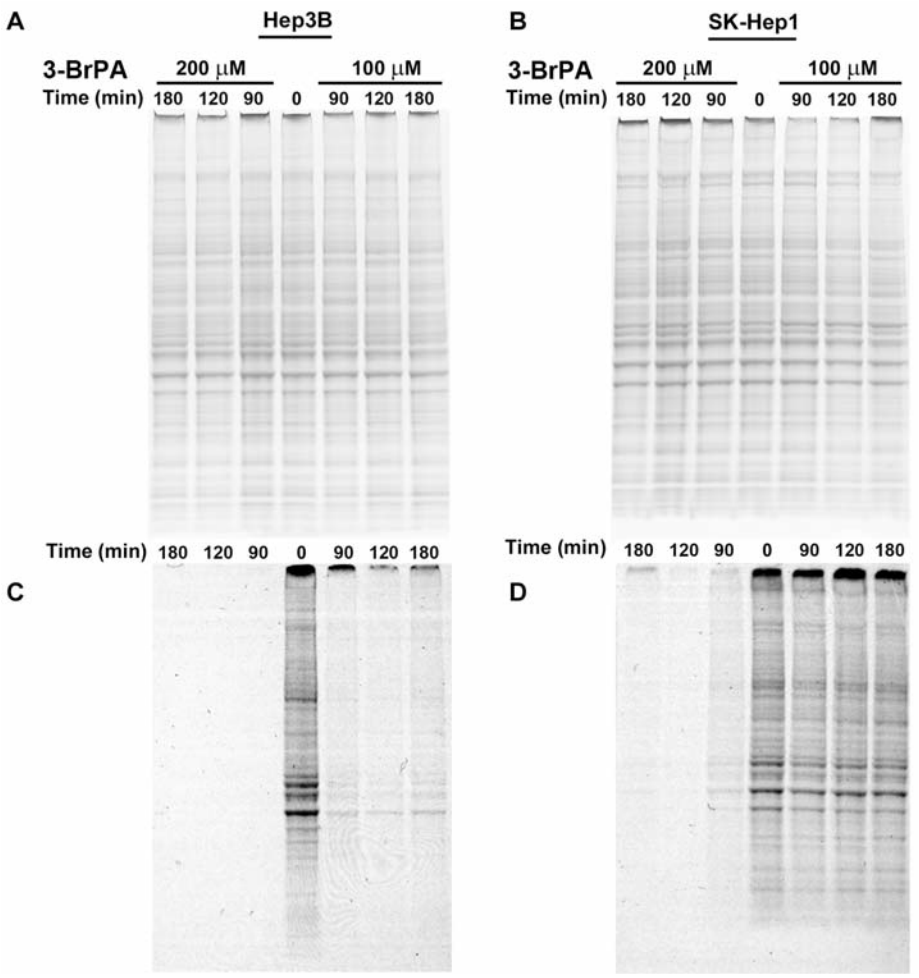


Figure 3. *Effect of 3-BrPA treatment on global protein synthesis (translation). Translation inhibition shown by pulse experiment with [$^{35}$S] methionine. Coomassie-stained gels of Hep3B (A) and SK-Hep1 (B) cells showing equal protein loading and their corresponding autoradiograms (C, D) for the newly synthesized proteins. Note: Hep3B cells show translation inhibition at a lower concentration of 3-BrPA (100 μM) than SK- Hep1 cells (200 μM).*

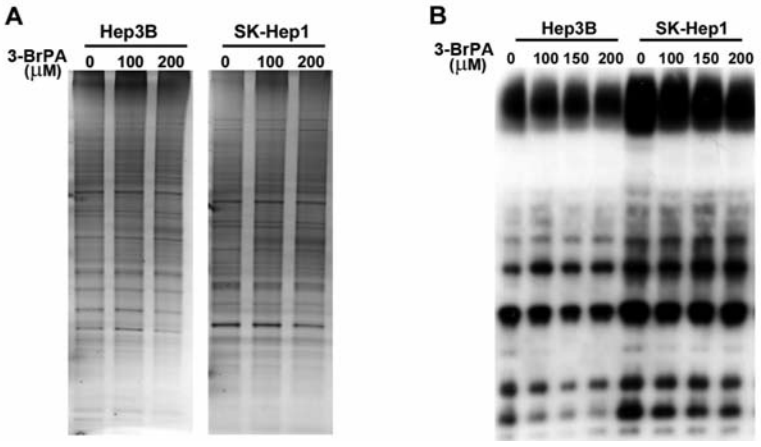


Figure 4. *Effect of 3-BrPA treatment on total protein depletion is not due to degradation. A: Silver- stained SDS-PAGE gels of lysates from equal number of cells treated with or without 3-BrPA. Hep3B and SK-Hep1 cell lysates showed depletion in the total protein profiles upon 3-BrPA treatment. B: 3-BrPA-mediated decrease in total cellular protein is not due to ubiquitin related proteasomal degradation. Immunoblot of Hep3B and SK-Hep1 cell lysates treated with different concentrations of 3-BrPA showed no increase in the amount of ubiquitinated proteins.*

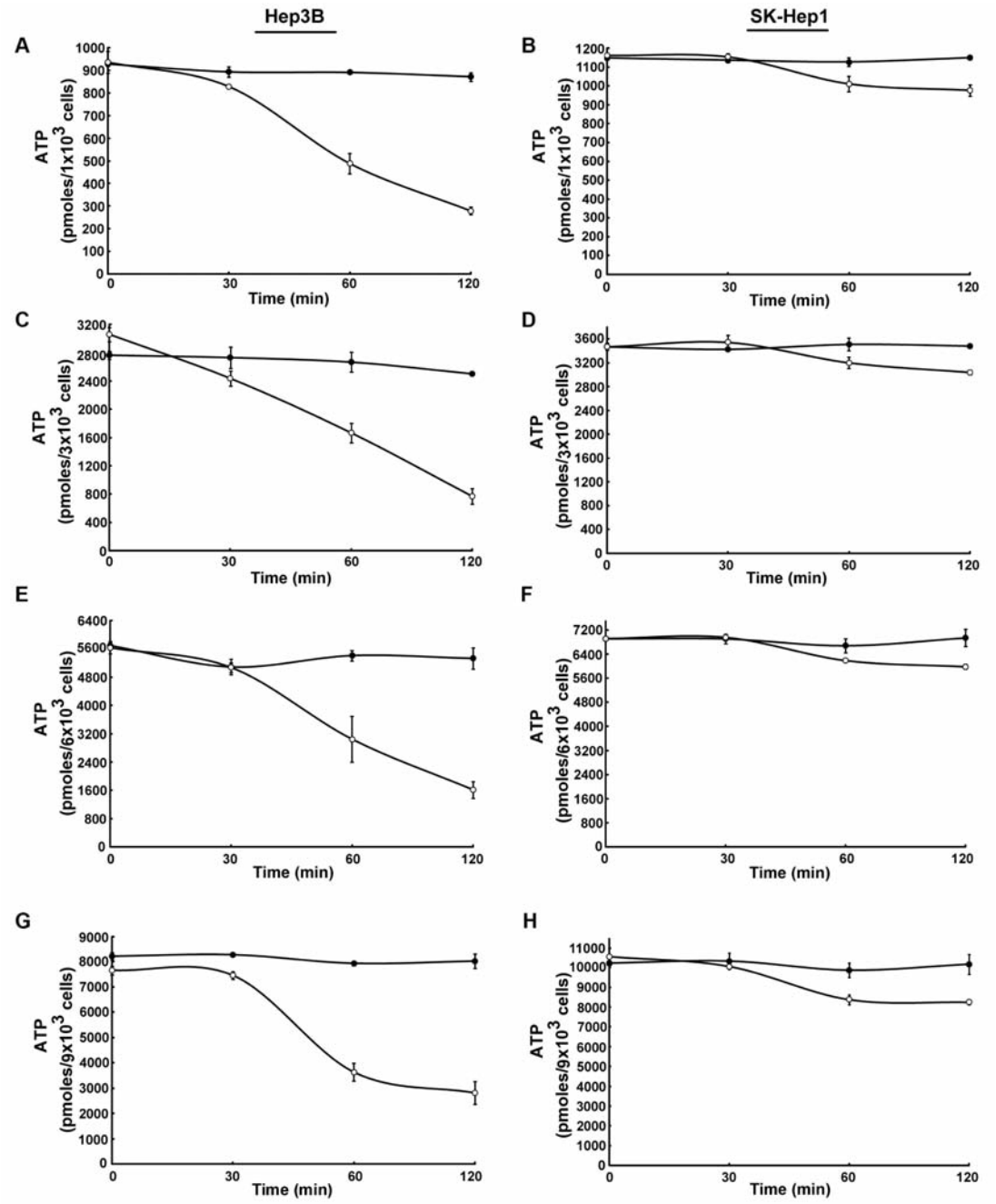


Figure 5. *3-BrPA-mediated translation inhibition is not dependent on ATP depletion. Hep3B cells showed a sustained ATP depletion only at 200 μM 3-BrPA but not at 100 μM for various cell numbers (A, C, E, G). Note: Translation inhibition was evident even at 100 μM 3-BrPA treatment (see Figure 3C). SK-Hep1 cells also showed a decrease in ATP molecules only at 200 μM 3-BrPA, but not at 100 μM, irrespective of the cell numbers (B, D, F, H). Solid circle represents 100 μM 3-BrPA and open circle represents 200 μM 3-BrPA treatment. Note: ATP depletion in SK-Hep1 cells is less than <20% even at 200 μM 3-BrPA, however the translation inhibition is prominent at the same condition.*

ribosomal proteins in both the cell lines (Figure 1A, B). Comparatively, Hep3B cells showed an earlier onset of cellular stress (at 100 μM 3-BrPA) than SK-Hep1 cells. Next, we specifically tested the effect of 3-BrPA treatment on the ER stress. Hep3B cells showed an increase (between 2 and 4-fold) in the expression of ER stress marker genes such as *ATF4, CHOP* and *GADD34* (Figure 1C) during 100 μM 3-BrPA treatment, whereas SK-Hep1 cells showed no marked difference under the same conditions (Figure 1D). At a higher dose of 3-BrPA (200 μM) Hep3B cells exhibited a

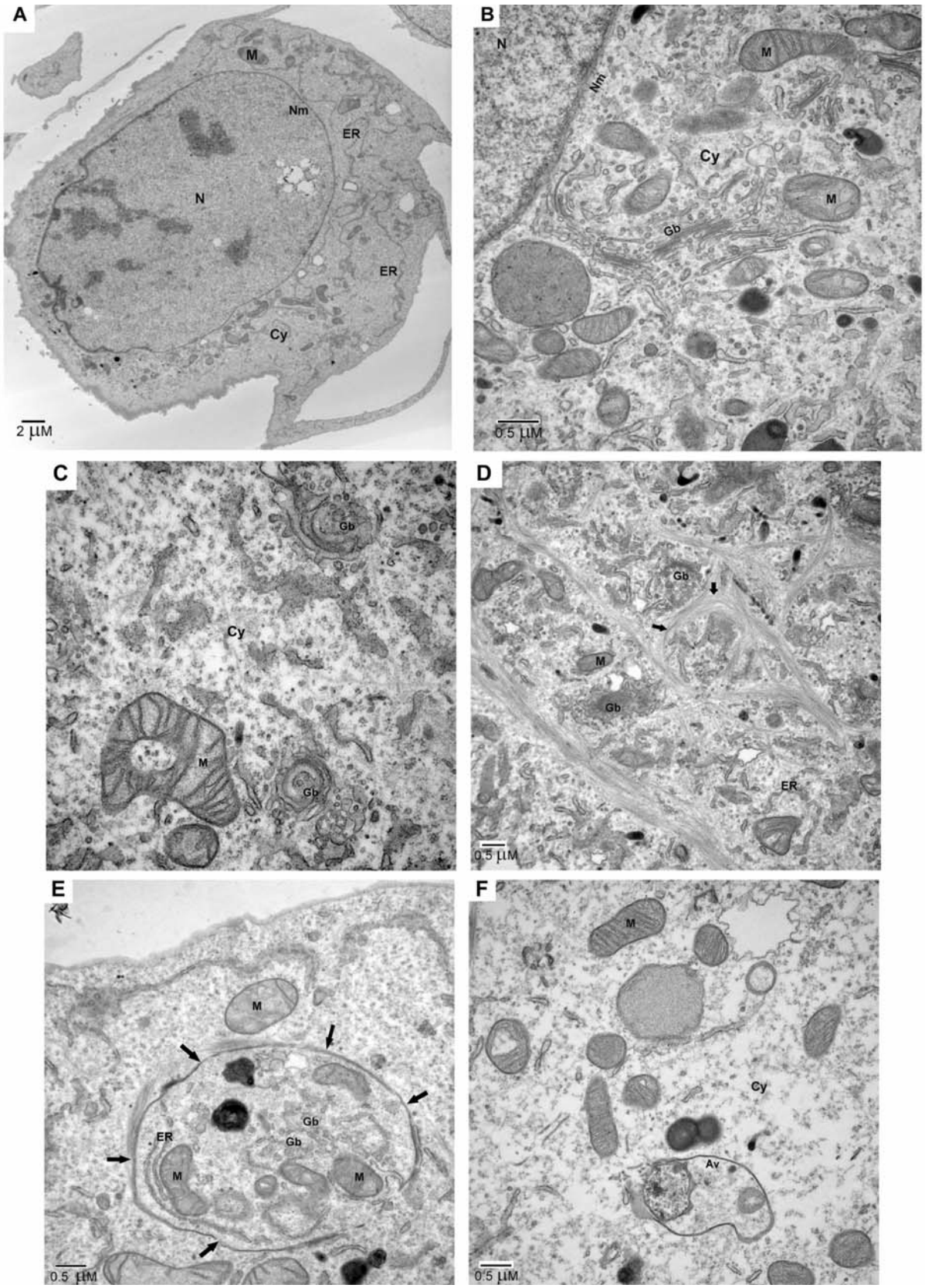


Figure 6. *continued*

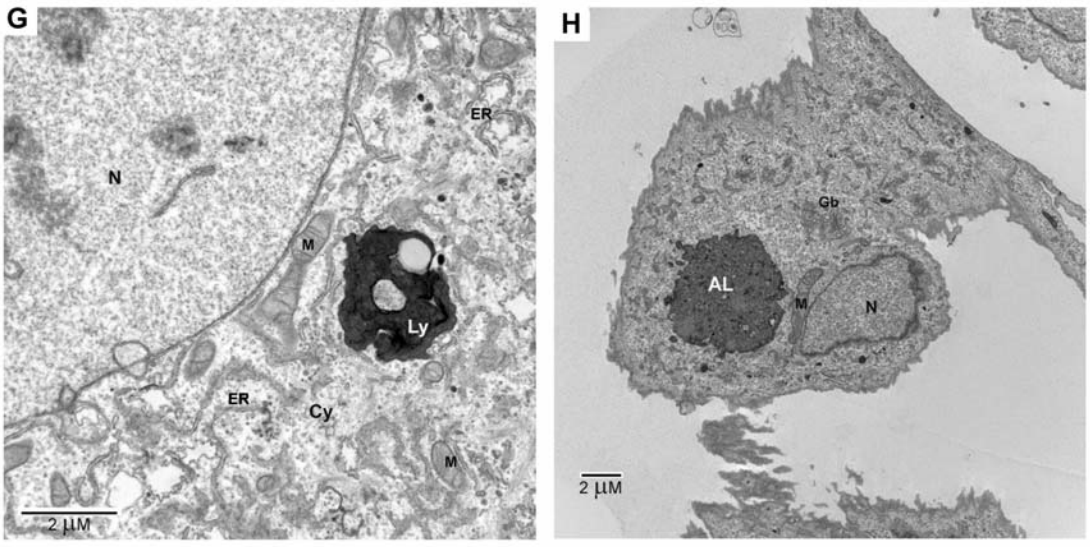


Figure 6. *Electron micrographs of Hep3B cells showing ultrastructural details. A: Hep3B cell (control) showing a typical large nucleus (N) with prominent heterochromatin and the nuclear membrane (Nm). The cytoplasm (Cy) shows intact endoplasmic reticulum (ER), mitochondria (M) and other cytoplasmic organelles. B: Higher magnification of control cell showing the nucleo (N)-cytoplasmic (Cy) region containing intact nucleus (N), nuclear membrane (Nm), Golgi bodies (Gb) and mitochondria (M). C-H: Hep3B cell treated with 3-BrPA (150 µM for 120 min) showing the ultrastructural changes. Disintegrated Golgi bodies (Gb), amorphous cytoplasm (Cy) and distended mitochondria (M) can be seen. D: Higher magnification of the cytoplasmic region showing unusual disorganization of cytokeratin-like filamentous structures. E: Characteristic autophagosome formation (indicated by arrows) engulfing a part of cytoplasm and other organelles such as Golgi bodies (Gb), mitochondria (M) and endoplasmic reticulum (ER). F: Typical autophagosome vacuole (Av) in the process of engulfing cytoplasmic contents. G, H: Hep3B cells treated with 3-BrPA showing electron dense lysosome-like (Ly) and autophago-lysosome (AL)-like structures.*

significant increase in *ATF4* and *CHOP* (Figure 1C) whereas SK-Hep1 cells showed a 2.5- and 3.5-fold increase in the level of *GADD 34* and *CHOP* respectively (Figure 1D). The immunoblot analysis also confirmed 3-BrPA-dependent overexpression of *CHOP* in both Hep3B and SK-Hep1 cell lines (Figure 9). Together, these data indicated an earlier onset of ER stress in Hep3B cells as compared to SK-Hep1cells. Moreover, the immunoblot analysis revealed that 3-BrPA treatment induced a differential response in Hep3B and SK-Hep1 cells with respect to various ER stress markers. Both the cell lines demonstrated similar ER stress response as evident by the increased expression of phospho-PERK, PDI, calnexin and phospho-eIF2α. However, a marked difference in the level of IRE1α and Ero1 was also observed between the cell lines (Figure 2A, B; Figure 10).

*3-BrPA treatment initiated translation inhibition*. As phospho-eIF2α is an indicator of translation inhibition, we next investigated the effect of 3-BrPA treatment on the translation potential of these cell lines. The data obtained from pulse experiments indicated that 3-BrPA treatment completely inhibited translation in both Hep3B and SK-Hep1 cell lines (Figure 3A-D). Hep3B cells showed an early response of translation inhibition at a lower dose (100 µM of 3-BrPA) than that of SK-Hep1 cells (200 µM of 3-BrPA). The 3-BrPA-dependent decrease in the total cellular protein was also confirmed by silver-staining of SDS-PAGE gels loaded with proteins obtained from equal number of cells treated with and without 3-BrPA (Figure 4A). In order to establish that a decrease in total cellular protein after 3-BrPA treatment was not due to ubiquitin/proteasomal degradation, we performed immunoblotting for ubiquitination in 3-BrPA-treated cells and the results showed no difference between the control and 3-BrPA-treated cells in the level of ubiquitinated proteins. This implied that the decrease in protein level is not due to ubiquitin-dependent proteasomal degradation but perhaps due to factors yet to be identified (Figure 4B).

*3-BrPA-mediated translation inhibition is independent of ATP depletion*. We then investigated whether the 3-BrPA-mediated translation inhibition could be due to a change in level of intracellular ATP. The absolute quantification of intracellular ATP (Figure 5) showed that the total number of ATP moles decreased in a dose- and time-dependent manner in both the cell lines. This decrease in the absolute level of intracellular ATP showed a similar trend irrespective of the total number of cells plated (Figure 5A-H). Interestingly, as shown in Figure 3C, the translation inhibition in Hep3B cells began at 100 µM 3-BrPA treatment, a dose at which there

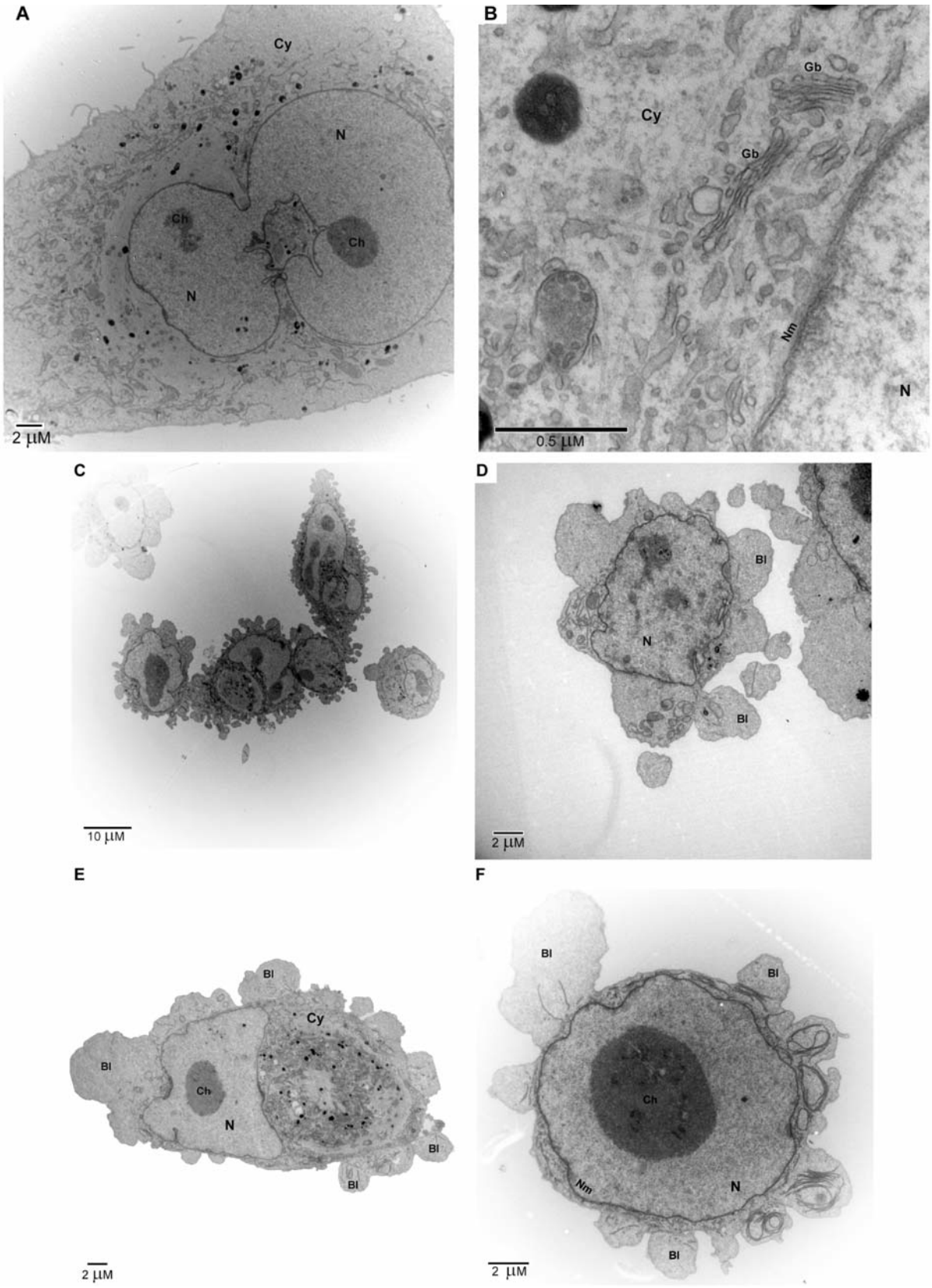


Figure 7. *continued*

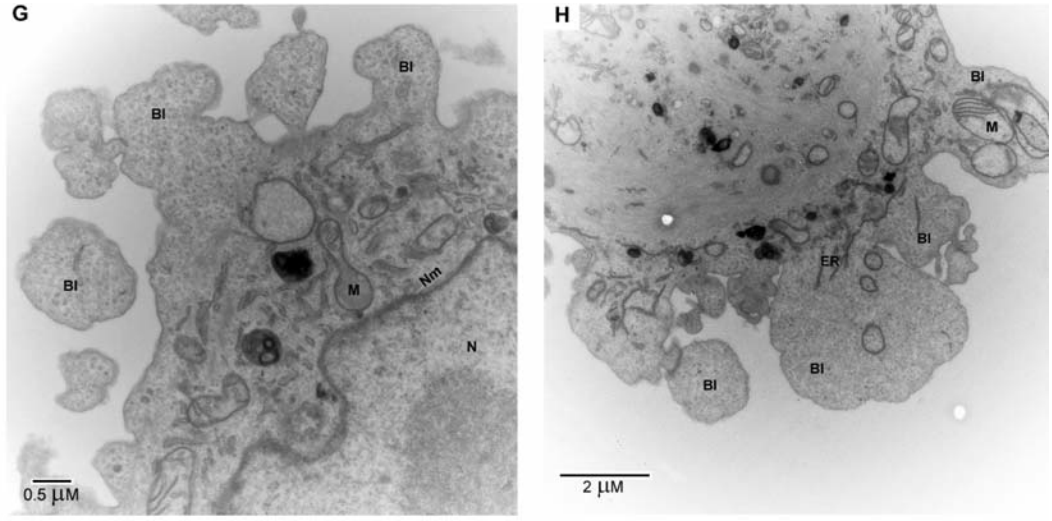


Figure 7. *Electron micrographs of SK-Hep1 cells showing ultrastructural details. A: SK-Hep1 cell (control) with typical large nucleus (N) with prominent heterochromatin (Ch). The cytoplasm (Cy) shows intact cytoplasmic organelles. The cell is in the stage of cell division showing karyokinesis. B: Higher magnification of control cell showing the nucleo (N)-cytoplasmic (Cy) region containing the nucleus (N), nuclear membrane (Nm) and intact Golgi bodies (Gb). C-H: SK-Hep1 cells treated with 3-BrPA (150 µM for 120 min) showing the ultrastructural changes and formation of multiple blebs (Bl). E: Enlargement of nucleus (N), pushing the cytoplasm (Cy) towards the periphery. (F) Enlargement of nucleus (N) with prominent chromatin (Ch) and nuclear membrane (Nm) in another SK-Hep1 cell. G: SK-Hep1 cell showing the blebbing and detached blebs. H: Typical bleb formation containing part of the cytoplasm and organelles such as mitochondria (M), endoplasmic reticulum (ER).*

was no significant decrease in the intracellular ATP level for different periods of treatment (Figure 5A, C, E, G). Thus, even before a substantial decrease in ATP level, the translation inhibition was in effect, perhaps due to the early onset of ER stress in Hep3B cells. Furthermore, for SK-Hep1 cells, the translation inhibition was evident only at 200 µM 3-BrPA treatment (Figure 3D), however the number of ATP moles depleted even at 120 min of 200 µM 3-BrPA treatment was <20% (Figure 5B, D, F, H). Thus, the translation inhibition induced by 3-BrPA treatment in both the cell lines was not dependent on the ATP depletion.

*3-BrPA induced autophagosome formation in Hep3B and apoptotic blebbing in SK-Hep1 cells*. As the translation inhibition and the expression of ER stress markers unequivocally demonstrated that 3-BrPA induced chronic ER stress, we investigated 3-BrPA-dependent ultrastructural changes in both the cell lines. Electron micrographs of an untreated Hep3B cell (control) show an intact ER and other organelles such as mitochondria, Golgi bodies *etc*., (Figure 6A, B). On the other hand, the electron micrographs of Hep3B cells treated with 3-BrPA exhibited a prominent change in organelles such as mitochondria, Golgi bodies and ER, with an amorphous cytoplasm (Figure 6C, D) and formation of double-membranous structures, the classical signature of autophagosome formation (Figure 6E, F) during the process of autophagy. Subsequently, sequestration of bulk of cytoplasm and organelles into double-membrane structures were also observed, with the appearance of electron-dense lysosome-like structures in 3-BrPA-treated Hep3B cells (Figure 6G, H). The electron micrographs of 3-BrPA-treated SK-Hep1 cells demonstrated the hallmark of apoptosis, *i.e*. blebbing which was absent in control or untreated cells (Figure 7A, B). A multiple number of blebs at different stages of formation with nuclear and cytoplasmic condensation were seen in many cells (Figure 7C-H). The formation of apoptotic bodies, a late event in the apoptotic process, was also observed (Figure 7C-H). In comparison, Hep3B cell did not show any such apoptotic bodies instead showed phagocytic ultrastructures and double membranous autophagosomes, typical markers of phagocytosis or autophagy. In order to confirm the observation of autophagosomes in 3-BrPA-treated Hep3B cells, we investigated the up-regulation of autophagy markers during 3-BrPA treatment in both the cell lines. The immunoblot analysis showed an increased expression of ATG5, ATG7 and also the conversion/degradation of LC3-I in Hep3B cells, confirming the event of autophagy (Figure 8A). In contrast, SK-Hep1 cells showed no significant change in the conversion/degradation of LC3-I, despite an increase in ATG5 and ATG7 (Figure 8A).

*3-BrPA treatment induced apoptosis in both HCC cell lines*. Finally, we attempted to identify the major pathway responsible for the cell death upon treatment with 3-BrPA in both Hep3B and SK-Hep1 cell lines. The immunoblot

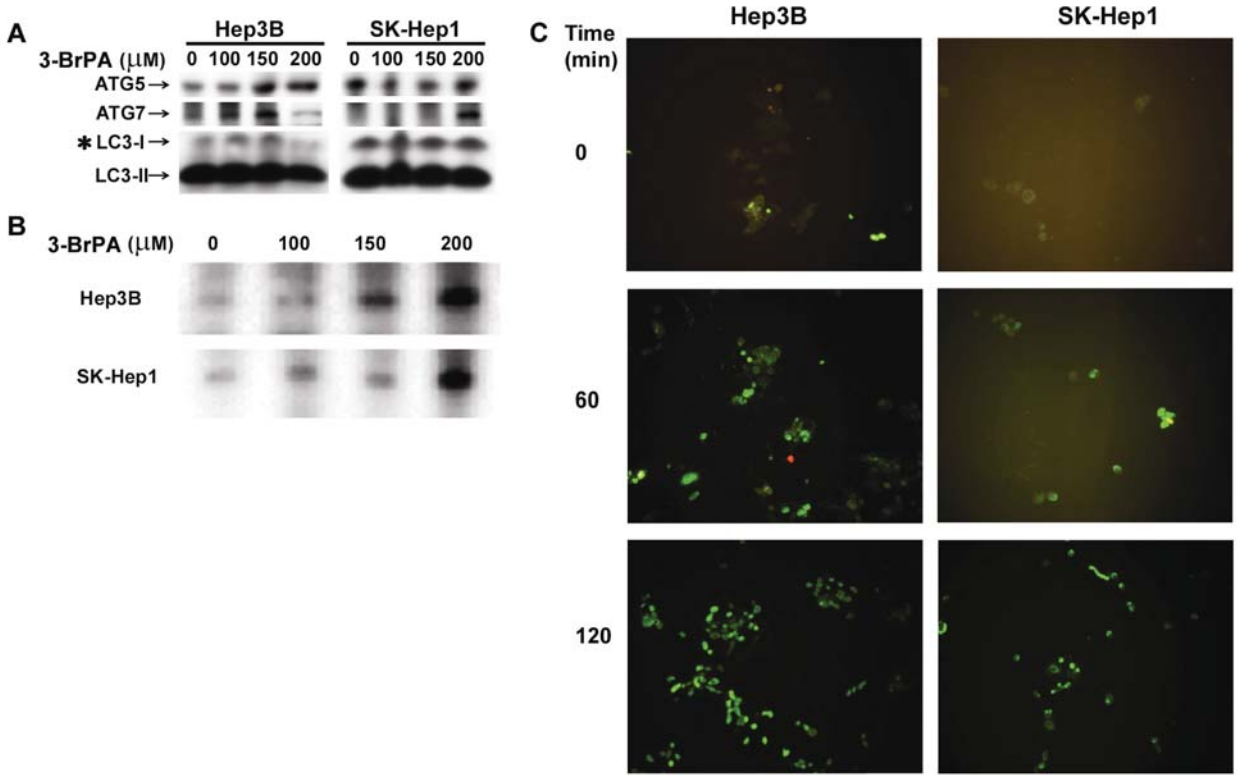


Figure 8. *3-BrPA treatment promotes apoptosis despite the induction of autophagy markers. A: Immunoblot showing induction of autophagy markers such as ATG5 and ATG7 in Hep3B and SK-Hep1 cells. However, the disappearance of LC3-I (*) an indicator of complete autophagy, is evidenced only in Hep3B cells but not in SK-Hep1 cells. B: 3-BrPA treatment induced a dose-dependent increase in the formation of active caspase-3 in both Hep3B and SK-Hep1 cell lines. Equal loading was achieved by loading protein lysates obtained from an equal number of cells. C: 3-BrPA treated (150 μM) Hep3B and SK-Hep1 cells show positive staining in the TUNEL assay.*

analysis showed a dose-dependent increase in the active (cleaved) caspase-3 (Figure 8B) and the TUNEL assay showed a time-dependent increase in the number of apoptotic cells in both Hep3B and SK-Hep1 cell lines (Figure 8C). Together these data demonstrated that 3-BrPA treatment promoted apoptosis eventually in both the cell lines despite the initial autophagic response of Hep3B cells.

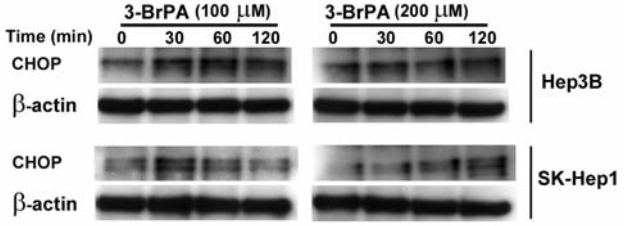


Figure 9. *3-BrPA treatment increased the expression of ER stress marker CHOP in a time- dependent manner in HCC cell lines. Immunoblots showing the increase in CHOP expression in Hep3B and SK-Hep1 cell lines in a time-dependent manner. Note: The prominent overexpression of CHOP in Hep3B at 100 μM 3-BrPA whereas in SK-Hep1 cells the increase is evident only at 200 μM 3-BrPA.*

## Discussion

The alkylating agent 3-BrPA has been shown to have a potent antitumor activity against liver cancer models with minimal toxicity to normal hepatic parenchyma at the therapeutic dose (25). We recently reported that 3-BrPA primarily targets the glycolytic enzyme GAPDH to cause apoptosis in HCC cell lines (20). In addition to its glycolytic function, a number of studies have identified the role of GAPDH in diverse cellular functions. Some of the common non-glycolytic functions of GAPDH include fusogenic properties (membrane fusion), membrane transport between the endoplasmic reticulum and the Golgi complex, tubulin bundling and cytoskeletal dynamics. GAPDH also interacts with nucleic acids, and has been known for its high affinity to transfer RNA (tRNA). In the context of apoptosis, the nuclear accumulation of GAPDH precedes apoptotic features that are antagonized by the overexpression of Bcl-2. The role of GAPDH in the nucleus includes the transcriptional regulation of several genes and

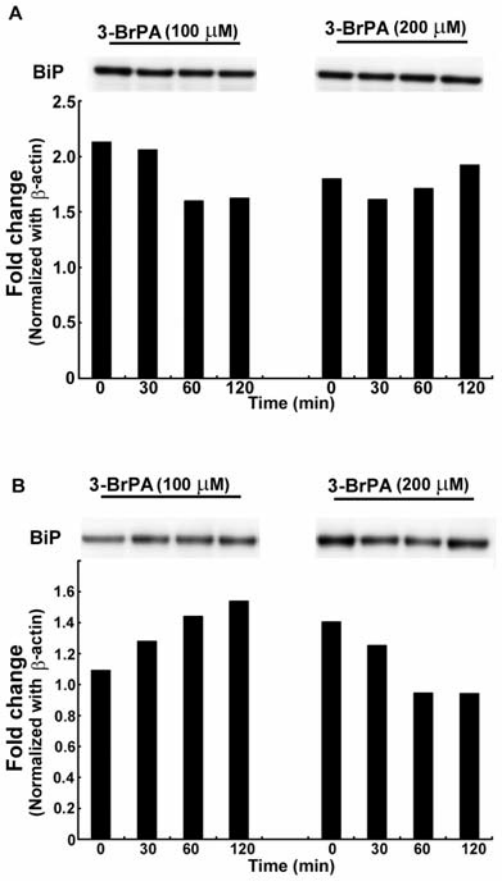


Figure 10. *ER stress induced by 3-BrPA-treatment could not be rescued by the chaperone BiP. A: Immunoblots showing Hep3B cells treated with 3-BrPA for different time intervals showing no significant increase in the expression of BiP implying the failure of rescue mechanism in 3-BrPA- treatment. B: Immunoblots of SK-Hep1 cells showing an initial increase (at 100 μM) in BiP yet could not sustain at higher concentration. This demonstrates that in SK-Hep1 cells the ER stress is sutained at 100 μM 3-BrPA (perhaps by BiP) but failed to protect at 200 μM 3-BrPA. Bottom panel indicates the densitometry quantitation of BiP normalized with β-actin.*

DNA repair (26, 27). GAPDH is also linked to apoptosis and autophagy in cancer cells with different genotypes (28). We have identified that 3-BrPA formed an irreversible bond with GAPDH and caused apoptosis in multiple HCC cell lines. Since the expression of the two major apoptotic proteins (p53, Fas) differ in Hep3B (null) and SK-Hep1 (wild-type) cell, we investigated the intracellular response of these cell lines to 3-BrPA treatment. It is quite evident from the data that the 3-BrPA treatment overcomes the cellular protective mechanism such as autophagy and triggers apoptosis even in p53/Fas-deficient HCC cell line, Hep3B. Our data indicated that 3-BrPA caused apoptosis in both the HCC cell lines regardless of their different genotype making it as an efficient anticancer agent to treat heterogeneous solid liver tumors.

The present data demonstrated that 3-BrPA induced ER stress in human HCC cell lines and the cellular response varied in terms of the early or late onset of ER stress. The induction of ER stress was through PERK-dependent pathway as evident from the increased level of phospho-PERK, phospho-eIF2α and their upstream targets such as CHOP and GADD 34 in both the cell lines. BiP is a well-known molecular chaperone that plays a critical role in mitigating ER stress and helping cells to recover. The data on BiP expression level indicated that Hep3B did not facilitate BiP-mediated chaperonic activity, whereas SK-Hep1 cells showed an initial induction (at 100 μM 3-BrPA) that failed to sustain (Figure 10). Together these data suggest that ER stress is more severe in Hep3B cells than in SK-Hep1 cells and the absence of BiP expression indicates a lack of chaperonic activity.

Hep3B cells exhibited severe ER stress (even at 100 μM 3-BrPA) and progressed towards a defensive cellular response, autophagy. Autophagy is a metabolic stress response and represents a key pathway for cellular adaptation and resistance. It involves the sequestration of intracellular components such as organelles and a part of the cytoplasm into double-membrane structures called autophagic vacuoles or autophagosomes leading to subsequent degradation by the lysosome. Moreover, some cancer cells when stressed with metabolic alterations such as energy depletion (amino acids, glucose) or hypoxia, activate autophagy as a protective response, in order to use the degraded or digested products to fuel necessary cellular processes for their survival (29, 30).

In Hep3B cells, autophagic response from ER stress was confirmed by demonstrating increased expression of autophagic markers (such as ATG5, ATG7 and conversion/degradation of LC3-I) and the formation of classic double-membranous autophagosome. Although SK-Hep1 cells showed 3-BrPA induced expression of ATG5 and ATG7, the lack of LC3-I conversion/ degradation and the absence of autophagosome under EM implied abrogation of autophagy. This corroborates with previous reports where cytoplasmic p53 has been shown to suppress autophagy (31, 32). It is noteworthy that p53 is expressed in SK-Hep1 cells but Hep3B cells are *p53* null.

Several anticancer chemotherapeutics have been shown to induce ER stress (33-36). In fact, it has been suggested that the use of two or more chemotherapeutics in any treatment protocol is necessary to induce ER stress severe enough to cause efficient tumor cell death (37). In addition, treatment with chemotherapeutics against some genotypes (p53/Fas deficient) of cancer cells causes progression to a protective autophagic response leading to resistance (38, 39). 3-BrPA is the first metabolic inhibitor that is shown here to cause apoptosis despite the existence of a protective cellular response such as autophagy in Hep3B cells. The critical role

of the ER stress response as a protective function in tumor cell growth and survival especially at the core of the tumor, where the hypoxic tumor cells resist chemotherapy, is well documented (40, 41). Cancer cell response to ER stress consists of expression of chaperones, antioxidants and/or progression to autophagy in order to rescue the cell from apoptosis. The efficacy of an anticancer agent to overcome these resistant responses is crucial in order to switch the cancer cell from its protective function to proapoptotic function, favoring cell death.

This study demonstrates that 3-BrPA is an effective agent in causing apoptosis in two distinct HCC cell lines, Hep3B and SK-Hep1. Hep3B cells lack key apoptotic regulators p53/Fas and hence respond by autophagy as a protective mechanism. However, this autophagy, which can be a cause of resistance to chemotherapy, is overcome by 3-BrPA treatment to cause apoptotic cell death. In the SK-Hep1 cells, which express both p53/Fas, 3-BrPA treatment causes ER stress leading to apoptosis *via* the classical pathway. This shows that 3-BrPA is effective in killing cancer cells over a broad range of genotypes, irrespective of the presence or absence of key regulatory proteins such as p53 or Fas. HCC tumors are highly heterogeneous and are commonly emerging from a background of chronic liver diseases such as alcoholic cirrhosis and chronic hepatitis B and C infections. Therefore, development of a therapeutic strategy that efficiently kills heterogeneous tumor is critical. Our data indicate that 3-BrPA is an efficient killer of tumor cells with a heterogeneous background, thus emphasizing its potential for clinical translation.

## Acknowledgements

This work was supported by the Abdulrahman Abdulmalik Research Fund (Jean-Francois Geschwind) and the Charles Wallace Pratt Research Fund (Jean-Francois Geschwind). We thank Ms. Carol Cooke for the help in electron microscopy studies (Figures 9, 10).

## Supporting Information Available

Immunoblots of CHOP and BiP from Hep3B and SK-Hep1 cells treated with 3-BrPA are provided as supporting data (Figures 9, 10).

## References

1 Hanahan D and Weinberg RA: The hallmarks of cancer. Cell *100(1)*: 57-70, 2000.

2 Hoyer-Hansen M and Jaattela M: Autophagy: An emerging target for cancer therapy. Autophagy *4(5)*: 574-580, 2008.

3 Maiuri MC, Tasdemir E, Criollo A, Morselli E, Vicencio JM, Carnuccio R and Kroemer G: Control of autophagy by oncogenes and tumor suppressor genes. Cell Death Differ *16(1)*: 87-93, 2009.

4 Carew JS, Nawrocki ST and Cleveland JL: Modulating autophagy for therapeutic benefit. Autophagy *3(5)*: 464-467, 2007.

5 Hoyer-Hansen M and Jaattela M: Connecting endoplasmic reticulum stress to autophagy by unfolded protein response and calcium. Cell Death Differ *14(9)*: 1576-1582, 2007.

6 Xu C, Bailly-Maitre B and Reed JC: Endoplasmic reticulum stress: Cell life and death decisions. J Clin Invest *115(10)*: 2656-2664, 2005.

7 Egger L, Schneider J, Rheme C, Tapernoux M, Hacki J and Borner C: Serine proteases mediate apoptosis-like cell death and phagocytosis under caspase-inhibiting conditions. Cell Death Differ *10(10)*: 1188-1203, 2003.

8 Ogata M, Hino S, Saito A, Morikawa K, Kondo S, Kanemoto S, Murakami T, Taniguchi M, Tanii I, Yoshinaga K, Shiosaka S, Hammarback JA, Urano F and Imaizumi K: Autophagy is activated for cell survival after endoplasmic reticulum stress. Mol Cell Biol *26(24)*: 9220-9231, 2006.

9 Bernales S, McDonald KL and Walter P: Autophagy counterbalances endoplasmic reticulum expansion during the unfolded protein response. PLoS Biol *4(12)*: e423, 2006.

10 Levine B and Kroemer G: Autophagy in the pathogenesis of disease. Cell *132(1)*: 27-42, 2008.

11 Llovet JM and Bruix J: Molecular targeted therapies in hepatocellular carcinoma. Hepatology *48(4)*: 1312-1327, 2008.

12 Parkin DM, Bray F, Ferlay J and Pisani P: Global cancer statistics, 2002. CA Cancer J Clin *55(2)*: 74-108, 2005.

13 Minguez B, Tovar V, Chiang D, Villanueva A and Llovet JM: Pathogenesis of hepatocellular carcinoma and molecular therapies. Curr Opin Gastroenterol *25(3)*: 186-194, 2009.

14 Stahler F and Roemer K: Mutant p53 can provoke apoptosis in p53-deficient Hep3B cells with delayed kinetics relative to wild-type p53. Oncogene *17(26)*: 3507-3512, 1998.

15 Lamboley C, Bringuier AF, Camus E, Lardeux B, Groyer A and Feldmann G: Overexpression of the mouse Fas gene in human Hep3B hepatoma cells overcomes their resistance to fas-mediated apoptosis. J Hepatol *36(3)*: 385-394, 2002.

16 Muller M, Strand S, Hug H, Heinemann EM, Walczak H, Hofmann WJ, Stremmel W, Krammer PH and Galle PR: Drug-induced apoptosis in hepatoma cells is mediated by the CD95 (APO-1/Fas) receptor/ligand system and involves activation of wild-type p53. J Clin Invest *99(3)*: 403-413, 1997.

17 Hsu SL, Chen MC, Chou YH, Hwang GY and Yin SC: Induction of p21(CIP1/Waf1) and activation of p34(cdc2) involved in retinoic acid-induced apoptosis in human hepatoma Hep3B cells. Exp Cell Res *248(1)*: 87-96, 1999.

18 Geschwind JF, Ko YH, Torbenson MS, Magee C and Pedersen PL: Novel therapy for liver cancer: Direct intraarterial injection of a potent inhibitor of ATP production. Cancer Res *62(14)*: 3909-3913, 2002.

19 Ko YH, Pedersen PL and Geschwind JF: Glucose catabolism in the rabbit VX2 tumor model for liver cancer: Characterization and targeting hexokinase. Cancer Lett *173(1)*: 83-91, 2001.

20 Ganapathy-Kanniappan S, Geschwind JF, Kunjithapatham R, Buijs M, Vossen JA, Tchernyshyov I, Cole RN, Syed LH, Rao PP, Ota S and Vali M: Glyceraldehyde-3-phosphate dehydrogenase (GAPDH) is pyruvylated during 3-bromopyruvate-mediated cancer cell death. Anticancer Res *29(12)*: 4909-4918, 2009.

21 Pereira da Silva AP, El-Bacha T, Kyaw N, dos Santos RS, da-Silva WS, Almeida FC, Da Poian AT and Galina A: Inhibition of energy-producing pathways of HepG2 cells by 3-bromopyruvate. Biochem J *417(3)*: 717-726, 2009.

22 Colell A, Green DR and Ricci JE: Novel roles for GAPDH in cell death and carcinogenesis. Cell Death Differ *16(12)*: 1573-1581, 2009.
23 Sirover MA: Role of the glycolytic protein, glyceraldehyde-3-phosphate dehydrogenase, in normal cell function and in cell pathology. J Cell Biochem *66(2)*: 133-140, 1997.
24 Neuhoff V, Arold N, Taube D and Ehrhardt W: Improved staining of proteins in polyacrylamide gels including isoelectric focusing gels with clear background at nanogram sensitivity using Coomassie brilliant blue G-250 and R-250. Electrophoresis *9(6)*: 255-262, 1988.
25 Vali M, Liapi E, Kowalski J, Hong K, Khwaja A, Torbenson MS, Georgiades C and Geschwind JF: Intraarterial therapy with a new potent inhibitor of tumor metabolism (3-bromopyruvate): Identification of therapeutic dose and method of injection in an animal model of liver cancer. J Vasc Interv Radiol *18(1 Pt 1)*: 95-101, 2007.
26 Sirover MA: New nuclear functions of the glycolytic protein, glyceraldehyde-3-phosphate dehydrogenase, in mammalian cells. J Cell Biochem *95(1)*: 45-52, 2005.
27 Meyer-Siegler K, Rahman-Mansur N, Wurzer JC and Sirover MA: Proliferative-dependent regulation of the glyceraldehyde-3-phosphate dehydrogenase/uracil DNA glycosylase gene in human cells. Carcinogenesis *13(11)*: 2127-2132, 1992.
28 Colell A, Ricci JE, Tait S, Milasta S, Maurer U, Bouchier-Hayes L, Fitzgerald P, Guio-Carrion A, Waterhouse NJ, Li CW, Mari B, Barbry P, Newmeyer DD, Beere HM and Green DR: GAPDH and autophagy preserve survival after apoptotic cytochrome *c* release in the absence of caspase activation. Cell *129(5)*: 983-997, 2007.
29 Lum JJ, DeBerardinis RJ and Thompson CB: Autophagy in metazoans: Cell survival in the land of plenty. Nat Rev Mol Cell Biol *6(6)*: 439-448, 2005.
30 Levine B and Klionsky DJ: Development by self-digestion: Molecular mechanisms and biological functions of autophagy. Dev Cell *6(4)*: 463-477, 2004.
31 Tasdemir E, Chiara Maiuri M, Morselli E, Criollo A, D'Amelio M, Djavaheri-Mergny M, Cecconi F, Tavernarakis N and Kroemer G: A dual role of p53 in the control of autophagy. Autophagy *4(6)*: 810-814, 2008.
32 Morselli E, Tasdemir E, Maiuri MC, Galluzzi L, Kepp O, Criollo A, Vicencio JM, Soussi T and Kroemer G: Mutant p53 protein localized in the cytoplasm inhibits autophagy. Cell Cycle *7(19)*: 3056-3061, 2008.
33 Fribley A, Zeng Q and Wang CY: Proteasome inhibitor PS-341 induces apoptosis through induction of endoplasmic reticulum stress-reactive oxygen species in head and neck squamous cell carcinoma cells. Mol Cell Biol *24(22)*: 9695-9704, 2004.
34 Mimnaugh EG, Xu W, Vos M, Yuan X, Isaacs JS, Bisht KS, Gius D and Neckers L: Simultaneous inhibition of hsp 90 and the proteasome promotes protein ubiquitination, causes endoplasmic reticulum-derived cytosolic vacuolization, and enhances antitumor activity. Mol Cancer Ther *3(5)*: 551-566, 2004.
35 Carracedo A, Gironella M, Lorente M, Garcia S, Guzman M, Velasco G and Iovanna JL: Cannabinoids induce apoptosis of pancreatic tumor cells *via* endoplasmic reticulum stress-related genes. Cancer Res *66(13)*: 6748-6755, 2006.
36 Carracedo A, Lorente M, Egia A, Blazquez C, Garcia S, Giroux V, Malicet C, Villuendas R, Gironella M, Gonzalez-Feria L, Piris MA, Iovanna JL, Guzman M and Velasco G: The stress-regulated protein p8 mediates cannabinoid-induced apoptosis of tumor cells. Cancer Cell *9(4)*: 301-312, 2006.
37 Kardosh A, Golden EB, Pyrko P, Uddin J, Hofman FM, Chen TC, Louie SG, Petasis NA and Schonthal AH: Aggravated endoplasmic reticulum stress as a basis for enhanced glioblastoma cell killing by bortezomib in combination with celecoxib or its non-coxib analogue, 2,5-dimethyl-celecoxib. Cancer Res *68(3)*: 843-851, 2008.
38 Brenes O, Arce F, Gatjens-Boniche O and Diaz C: Characterization of cell death events induced by anti-neoplastic drugs cisplatin, paclitaxel and 5-fluorouracil on human hepatoma cell lines: Possible mechanisms of cell resistance. Biomed Pharmacother *61(6)*: 347-355, 2007.
39 Tam KH, Yang ZF, Lau CK, Lam CT, Pang RW and Poon RT: Inhibition of mTOR enhances chemosensitivity in hepatocellular carcinoma. Cancer Lett *273(2)*: 201-209, 2009.
40 Boyce M and Yuan J: Cellular response to endoplasmic reticulum stress: A matter of life or death. Cell Death Differ *13(3)*: 363-373, 2006.
41 Wu J and Kaufman RJ: From acute ER stress to physiological roles of the unfolded protein response. Cell Death Differ *13(3)*: 374-384, 2006.

*Received November 30, 2009*
*Revised January 28, 2010*
*Accepted January 28, 2010*